

Density of states near a vortex core in ferromagnetic superconductors: Application to STM measurements

Jacob Linder,¹ Takehito Yokoyama,² and Asle Sudbø¹

¹*Department of Physics, Norwegian University of Science and Technology, N-7491 Trondheim, Norway*

²*Department of Applied Physics, Nagoya University, Nagoya, 464-8603, Japan*

(Dated: Received November 29, 2018)

We investigate numerically the local density of states (LDOS) in the vicinity of a vortex core in a ferromagnetic superconductor. Specifically, we investigate how the LDOS is affected by the relative weight of the spin bands in terms of the superconducting pairing, and we also examine the effect of different pairing symmetries for the superconducting order parameter. Our findings are directly related to scanning tunneling microscopy measurements and may thus be highly useful to clarify details of the superconducting pairing in recently discovered ferromagnetic superconductors.

PACS numbers: 74.25.Op, 74.25.Ha

I. INTRODUCTION

Recently, UCoGe was added to the distinguished list of materials (already featuring UGe₂ and URhGe) which appear to display coexistence of ferromagnetism and superconductivity^{1,2,3}. While ferromagnetism and conventional superconductivity may be shown to be antagonistic in terms of a bulk coexistent state⁴, several studies have pointed out the possibility of a non-unitary, spin-triplet superconducting state coexisting with itinerant ferromagnetism^{5,6,7,8,9,10}. The synthesis of two important phenomena in condensed-matter physics, ferromagnetism and superconductivity, is not only interesting from the point of view of basic research, but has also spawned hope of potential applications in low-temperature nanotechnology.

A number of questions arise concerning the nature of the coexistence of ferromagnetic and superconducting order. In particular, it is crucial to address *i*) whether the two long-range orders are phase-separated or not, *ii*) whether the microscopic coexistence is spatially homogeneous or not, and *iii*) what the symmetry of the superconducting order parameter is. Concerning the first question, the answer clearly appears to be 'yes', since the onset of superconductivity appears inside the ferromagnetic part of the phase diagram⁶. The second question is, however, still open. Some authors have studied spatially uniform coexistence of ferromagnetic and superconducting order^{7,8,9,10,11}, while others have pointed out the intriguing possibility of a spontaneously formed vortex lattice state^{12,13,14}, due to the internal field. It has been argued¹⁵ that a key factor with regard to whether such a spontaneous vortex phase appears or not is the magnitude of the internal magnetization \mathbf{M} . Finally, although the issue of pairing symmetry raised in the third question has not been established conclusively, the most likely option appears to be a non-unitary, spin triplet superconducting state, where the spin of the Cooper pair couples to the bulk magnetization through a third order term $\sim \mathbf{d}_{\mathbf{k}} \times \mathbf{d}_{\mathbf{k}}^* \cdot \mathbf{M}$ in the Ginzburg-Landau free energy. Several studies^{16,17,18,19,20} have addressed means by which one may identify the pairing symmetry of the superconducting order parameter in a ferromagnetic superconductor, mainly focusing on transport properties.

Clearly, it would be highly desirable to clarify experimental signatures of a possible spontaneous vortex lattice-phase realized in a ferromagnetic superconductor. In this work, we present numerical results for the local density of states (LDOS) in the vicinity of a vortex-core of a ferromagnetic superconductor. Our approach is based on the quasiclassical theory of superconductivity, and takes into account several crucial factors such as the depletion of the order parameter near the vortex core in addition to self-consistently obtained magnetic and superconducting order parameters. Our results are directly relevant for scanning tunneling microscopy (STM) measurements,²¹ and may be useful to clarify signatures of the existence of a spontaneously formed vortex lattice and also the pairing symmetry of the superconducting order parameter.

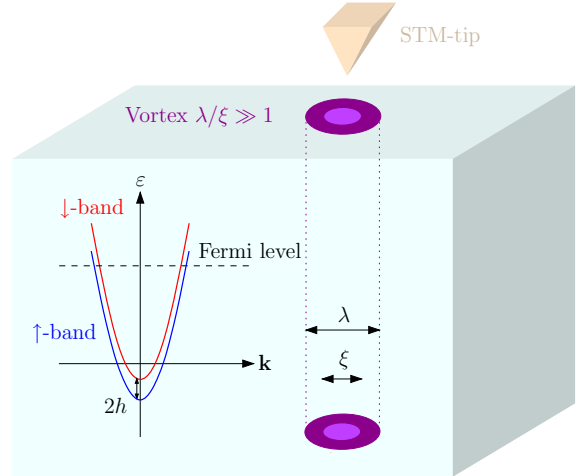


FIG. 1: (Color online) Schematic illustration of the model.

This paper is organized as follows. In Sec. II, we establish the theoretical framework employed in this work. Namely, we use the quasiclassical approximation and solve the Eilenberger equation in the vicinity of the vortex core with appropriate boundary conditions. In Sec. III, we present our results for the spatial- and energy-dependence of the local density of states near the vortex core. Specifically, we investigate how

the relative weight of the spin bands in terms of the superconducting pairing and different pairing symmetries for the superconducting order parameter affect the density of states. In Sec. IV and V, we discuss and summarize the main results of the paper. We will use boldface notation for 2-vectors, $\hat{\cdot}$ for 4×4 matrices, and $\underline{\cdot}$ for 2×2 matrices.

II. THEORETICAL FRAMEWORK

It is generally believed that the pairing symmetry in ferromagnetic superconductors may be classified as a non-unitary, spin-triplet state.^{5,7,8} Our starting point is the quasiclassical Eilenberger equation²² for such a system, which in the clean limit reads (see Appendix A for details)

$$\mathbf{v}_F \cdot \nabla \hat{g}^R + [\varepsilon \hat{\rho}_3 + \hat{M} + \hat{\Delta}(\mathbf{p}_F), \hat{g}^R] = 0, \quad (1)$$

where ε is the quasiparticle energy measured from the Fermi level, \mathbf{v}_F is the Fermi velocity, and $[\dots]$ is a commutator. The exchange field h and the superconducting order parameters Δ_σ are contained in the terms of $\hat{M} = h \text{diag}(\tau_3, \tau_3)$ in addition to

$$\begin{aligned} \hat{\Delta}(\mathbf{p}_F) &= \begin{pmatrix} 0 & \underline{\Delta}(\mathbf{p}_F) \\ -\underline{\Delta}^*(\mathbf{p}_F) & 0 \end{pmatrix}, \\ \underline{\Delta}(\mathbf{p}_F) &= \begin{pmatrix} \Delta_\uparrow(\mathbf{p}_F) & 0 \\ 0 & \Delta_\downarrow(\mathbf{p}_F) \end{pmatrix}. \end{aligned} \quad (2)$$

The matrices $\hat{\rho}_i$ and τ_i are defined in the Appendix. The retarded part of the Green's function, \hat{g}^R , will have the structure

$$\hat{g}^R = \begin{pmatrix} g(\mathbf{r}, \mathbf{p}_F, \varepsilon) & f(\mathbf{r}, \mathbf{p}_F, \varepsilon) \\ -f^*(\mathbf{r}, -\mathbf{p}_F, -\varepsilon) & -g^*(\mathbf{r}, -\mathbf{p}_F, -\varepsilon) \end{pmatrix},$$

and must satisfy the normalization condition $(\hat{g}^R)^2 = \hat{1}$. Due to the internal symmetry relations between the components of \hat{g}^R , one may parametrize it very conveniently by means of a so-called Ricatti-parametrization^{23,24}. In the absence of interband-scattering, the Eilenberger equation decouples into two 2×2 equations as follows:

$$\mathbf{v}_F \cdot \nabla \underline{g}_\sigma + [\varepsilon \tau_3 + \sigma h \tau_0 + \underline{\Delta}_\sigma(\mathbf{p}_F), \underline{g}_\sigma] = 0, \quad (3)$$

where we have introduced

$$\begin{aligned} \underline{g}_\sigma &= N_\sigma \begin{pmatrix} 1 - a_\sigma b_\sigma & 2a_\sigma \\ 2b_\sigma & -1 + a_\sigma b_\sigma \end{pmatrix}, \quad N_\sigma = (1 + a_\sigma b_\sigma)^{-1}, \\ \underline{\Delta}_\sigma(\mathbf{p}_F) &= \begin{pmatrix} 0 & \Delta_\sigma(\mathbf{p}_F) \\ -\Delta_\sigma^*(\mathbf{p}_F) & 0 \end{pmatrix}. \end{aligned} \quad (4)$$

Note that the gap matrix in Eq. (4) is a 2×2 matrix in particle-hole space, while the gap matrix in Eq. (2) is a 2×2 matrix in spin-space. From Eq. (3), one obtains two decoupled differential equations for a_σ and b_σ :

$$\begin{aligned} \mathbf{v}_F \cdot \nabla a_\sigma + 2a_\sigma \varepsilon - a_\sigma^2 \Delta_\sigma^*(\mathbf{p}_F) - \Delta_\sigma(\mathbf{p}_F) &= 0, \\ \mathbf{v}_F \cdot \nabla b_\sigma - 2b_\sigma \varepsilon - b_\sigma^2 \Delta_\sigma(\mathbf{p}_F) - \Delta_\sigma^*(\mathbf{p}_F) &= 0. \end{aligned} \quad (5)$$

Note that the above equations do not have any *explicit* dependence on the exchange splitting h . As we shall see later, the exchange splitting does however enter implicitly through the spin-dependent gaps Δ_σ . Note that the magnetic vector potential \mathbf{A} may be incorporated above simply by a shift in the quasiparticle energies: $\varepsilon \rightarrow \varepsilon + e\mathbf{v}_F \cdot \mathbf{A}$. In a gauge that renders the superconducting gaps to be real, one finds that $e\mathbf{A} \rightarrow e\mathbf{A} - \nabla\Phi/2$, where Φ is the superconducting phase associated with the broken U(1) symmetry. Therefore, the total Doppler shift in the quasiparticle energies is $\varepsilon \rightarrow \varepsilon - em\mathbf{v}_F \cdot \mathbf{v}_s$, where the gauge-invariant superfluid velocity is $\mathbf{v}_s = (\nabla\Phi - 2e\mathbf{A})/(2m)$. Below, we keep the distribution of the superconducting phase in the order parameter and consider the case with Ginzburg-Landau parameter $\kappa \gg 1$, for which the magnetic vector potential \mathbf{A} may be neglected. This follows since we are considering only one single vortex, i.e. the zero-field limit, such that only gauge-field fluctuations around zero could possibly be relevant. However, assuming that the superconductors are strongly type-II with $\kappa \gg 1$, gauge-field fluctuations are suppressed^{25,26}.

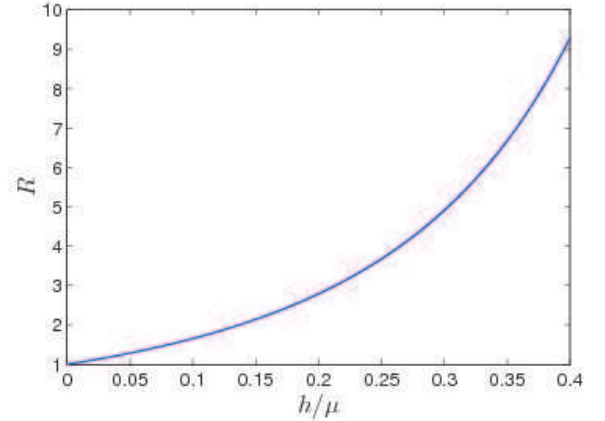


FIG. 2: (Color online) The ratio R between the majority- and minority-spin gaps as a function of h/μ as obtained from a self-consistent, mean-field solution [Eq. (15)].

In order to solve the above Ricatti-equations, we follow closely the procedure of Ref. 23. Let us consider the term with $\mathbf{v}_F \cdot \nabla$ in more detail. Assume that we have a cylindrically symmetric vortex situated at $r_a = r_b = 0$ with its axis along $\hat{\mathbf{c}}$. The position vector in this coordinate system then reads $\mathbf{r} = r_a \hat{\mathbf{a}} + r_b \hat{\mathbf{b}}$. Assuming that the transport of quasiparticles primarily takes place in the $\hat{\mathbf{a}} - \hat{\mathbf{b}}$ -plane, we may define the Fermi velocity as

$$\mathbf{v}_F = v_F(\cos\theta \hat{\mathbf{a}} + \sin\theta \hat{\mathbf{b}}) \equiv v_F \hat{\mathbf{v}} \quad (6)$$

and its orthogonal vector $\hat{\mathbf{u}} = -\sin\theta \hat{\mathbf{a}} + \cos\theta \hat{\mathbf{b}}$. Thus, the position vector \mathbf{r} may also be expressed as $\mathbf{r} = x\hat{\mathbf{v}} + y\hat{\mathbf{u}}$, where we have defined

$$x = r_a \cos\theta + r_b \sin\theta, \quad y = -r_a \sin\theta + r_b \cos\theta. \quad (7)$$

Using the new coordinate system $\hat{\mathbf{v}} - \hat{\mathbf{u}}$, the Ricatti equations

may be rewritten as

$$\begin{aligned} i v_F \partial_x a_\sigma + [2\varepsilon - \Delta_\sigma^* a_\sigma] a_\sigma - \Delta_\sigma &= 0, \\ i v_F \partial_x b_\sigma - [2\varepsilon + \Delta_\sigma b_\sigma] b_\sigma - \Delta_\sigma^* &= 0, \end{aligned} \quad (8)$$

where $a_\sigma = a_\sigma(x, y)$ and $\Delta_\sigma = \Delta_\sigma(x, y)$. The above equations may be solved by imposing boundary conditions for $\{a_\sigma, b_\sigma\}$ in the bulk of the superconductor. The Riccati-equations with $\varepsilon > 0$ for a_σ and b_σ are stable for integration from $x \rightarrow (-\infty)$ and $x \rightarrow \infty$, respectively (opposite for $\varepsilon < 0$).²³ The boundary conditions then read:

$$\begin{aligned} a_\sigma[x \rightarrow (-\infty)] &= (\varepsilon - \sqrt{\varepsilon^2 - |\Delta_\sigma|^2})/\Delta_\sigma^*, \\ b_\sigma(x \rightarrow \infty) &= -(\varepsilon - \sqrt{\varepsilon^2 - |\Delta_\sigma|^2})/\Delta_\sigma. \end{aligned} \quad (9)$$

The superconducting order parameter Δ_σ is now modelled in the presence of a vortex centered at $r_a = r_b = 0$. In general, the superconducting order parameter may be written as²⁷

$$\Delta_\sigma(\mathbf{r}, \theta, \varepsilon) = \Delta_{\sigma,0} \chi_\sigma(\theta, \varepsilon) F(r) e^{im\phi}, \quad (10)$$

assuming a vorticity m . Here, Δ_0 is the gap magnitude, $\chi(\theta, \varepsilon)$ is a symmetry factor for the gap (taking into account both anisotropy and frequency-dependence), $F(r)$ models the spatial depletion of the gap near the vortex core, while $\tan \phi = r_b/r_a$. We will here restrict our attention to an even-frequency, p -wave symmetry, which is believed to be the most likely candidate for the order parameter in ferromagnetic superconductors. Assuming that the angular symmetry is the same for both the majority and minority spin gaps and considering the usual case of $m = 1$, we explicitly have

$$\Delta_\sigma(\mathbf{r}, \theta) = \Delta_{\sigma,0} \chi(\theta) \tanh\left(\frac{\sqrt{x^2 + y^2}}{\xi}\right) \frac{x + iy}{\sqrt{x^2 + y^2}}. \quad (11)$$

In what follows, we will compare the cases $\chi(\theta) = \cos \theta$ and $\chi(\theta) = e^{i\theta}$, and also investigate how the LDOS changes depending the relative weight of the superconducting instability in both spin-bands. The normalized LDOS for spin species σ is given by

$$N_\sigma(\mathbf{r}, \varepsilon) = \int_0^{2\pi} \frac{d\theta}{2\pi} \text{Re}\{(1 - a_\sigma b_\sigma)/(1 + a_\sigma b_\sigma)\}, \quad (12)$$

and we introduce the total LDOS in the standard way as

$$N(\mathbf{r}, \varepsilon) = \sum_\sigma N_\sigma(\mathbf{r}, \varepsilon)/2. \quad (13)$$

To account for a finite quasiparticle lifetime τ , we let $\varepsilon \rightarrow \varepsilon + i\delta$ where $\delta \sim \tau^{-1}$. From now on, we fix $\delta = 0.1\Delta_{\uparrow,0}$ and comment further upon the role of inelastic scattering in Appendix B.

Even if the exchange field h is absent from the Eilenberger equation, the LDOS is *not* independent of the value of h . The reason for this is that the magnitude of the superconducting gaps depend on the strength of the exchange splitting. Following the approach of Refs. 8,9, we derive from a weak-coupling

mean-field theory that the self-consistent solution of bulk superconducting gaps in the $T \rightarrow 0$ limit may be written as

$$\Delta_{\sigma,0}/\omega_0 = c \exp[-1/(g\sqrt{1 + \sigma h/\mu})], \quad (14)$$

where the prefactor is equal to $c \simeq 2.43$ for a p_x -wave symmetry [$\chi(\theta) = \cos \theta$], $c = 2.00$ for a chiral p -wave symmetry [$\chi(\theta) = e^{i\theta}$].^{8,9} Here, $g = V_0 N_0$ is the weak-coupling constant which we set to $g = 0.2$ and ω_0 is the typical frequency width around Fermi level for the bosons responsible for the superconducting pairing. Above, V_0 is the strength of the pairing interaction, N_0 is the LDOS at Fermi level in the normal-state and μ denotes the Fermi energy. The reader may consult Appendix C for a derivation of Eq. (14). We find that the ratio between the majority- and minority-spin gaps may be written as

$$\frac{\Delta_{\uparrow,0}}{\Delta_{\downarrow,0}} \equiv R(h/\mu) = \exp\left[\frac{\sqrt{1 + h/\mu} - \sqrt{1 - h/\mu}}{g\sqrt{1 - (h/\mu)^2}}\right] \quad (15)$$

when assuming that $h/\mu \in [0, 1]$ (shown in Fig. 2). In UGe₂, the energy splitting between the majority and minority spin bands was estimated² to lie around 70 meV, which yields $R \simeq 1.42$ when assuming $\mu = 1$ eV.

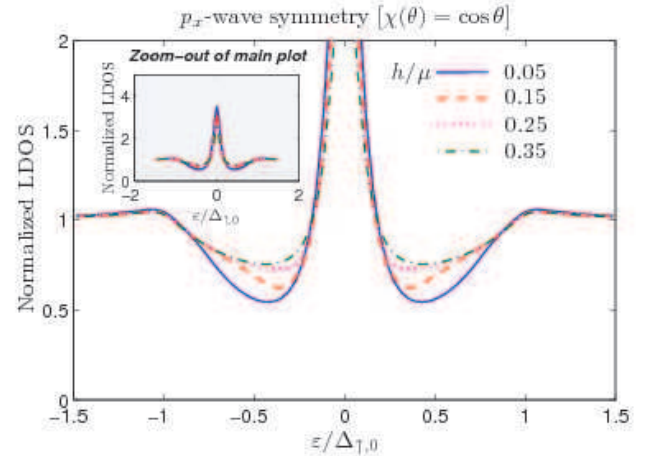


FIG. 3: (Color online) Normalized LDOS in the vortex core for a p_x -wave symmetry [$\chi(\theta) = \cos \theta$] using several values of h/μ .

III. RESULTS

We begin by plotting the energy-resolved LDOS in the vortex core ($r_a = r_b = 0$) for an order parameter which has line nodes in momentum space. Such an order parameter was recently proposed to be realized in UGe₂ by Harada *et al.*⁶, and it was moreover argued that the superconducting pairing only took place in the majority spin-band. To investigate how the relative magnitudes of the majority and minority spin gaps affect the LDOS in the vortex-core, we plot the LDOS for several values of the ratio h/μ in Fig. 3. As usual, the LDOS is strongly enhanced for subgap values due to the existence of

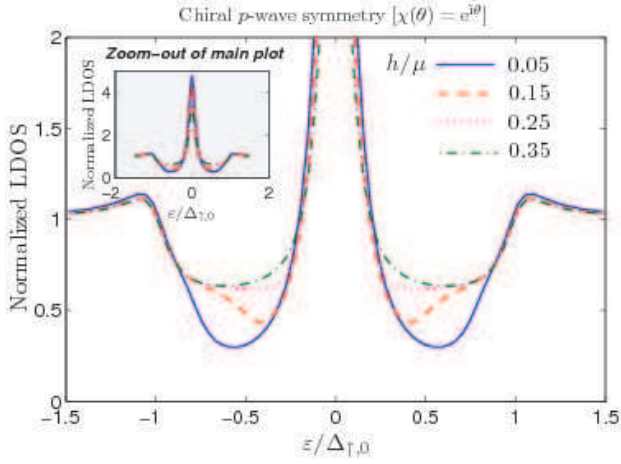


FIG. 4: (Color online) Normalized LDOS in the vortex core for a chiral p -wave symmetry [$\chi(\theta) = e^{i\theta}$] using several values of h/μ .

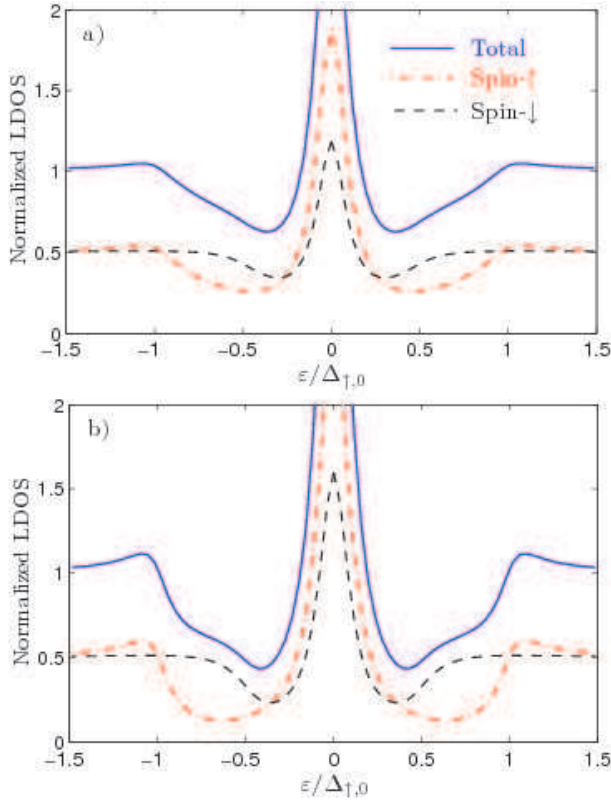


FIG. 5: (Color online) Total and spin-resolved LDOS in the vortex core for the a) p_x -wave symmetry [$\chi(\theta) = \cos \theta$] and the b) chiral p -wave symmetry [$\chi(\theta) = e^{i\theta}$]. We have here used $h/\mu = 0.15$.

bound states within the vortex core²⁸. The presence of two gaps in the system should manifest itself in the form of non-monotonous behaviour in the subgap spectrum, but it is not possible to discern such behaviour unambiguously from Fig. 3. This effect may be masked by strong inelastic scattering, modelled here by the parameter δ , which effectively smears

the LDOS. The effect of increasing the exchange field is seen to suppress the deviation from the normal-state LDOS. This may be understood by noting that the minority-spin gap is strongly reduced with increasing exchange field, and that the corresponding increase of the majority-spin gap is not able to compensate for the suppressed regime of bound states within the core.

We next study the chiral p -wave symmetry analogous to the A2-phase in liquid ^3He , and plot the energy-resolved LDOS for several values of h/μ in Fig. 4. Although the qualitative behaviour is quite similar to Fig. 3, there are two important distinctions. First, one notices that the chiral symmetry appears to have a much more pronounced influence on the LDOS quantitatively, yielding a larger zero energy-peak and larger subgap dips. This is in fact *opposite* what one would have expected from tunneling conductance measurements of p_x -wave and chiral p -wave superconductors, respectively. For such measurements, the zero-energy peak becomes much larger in the p_x -wave case than in the chiral p -wave case. Secondly, the subgap features associated with the presence of two gaps are enhanced in Fig. 4 compared to Fig. 3. The non-monotonous behaviour for subgap energies is present for all curves in Fig. 4, but the features indicative of multiple gaps are most clearly seen for $h/\mu = 0.15$, manifested through an additional inflection point before the normal state LDOS is recovered. These differences could be helpful in discriminating between different types of pairing symmetries in ferromagnetic superconductors.

In order to show more clearly the contribution from each spin-band to the LDOS near the vortex core, consider Fig. 5 where we plot the total LDOS and the contribution from each spin band for a) $\chi(\theta) = \cos \theta$ and b) $\chi(\theta) = e^{i\theta}$. The rise of the LDOS following the gap edge $\Delta_{\sigma,0}$ of each spin band occurs at different energies due to the exchange splitting. This is revealed in the total LDOS as kinks located at two distinct energies, which offers the opportunity to obtain explicit information about the relative magnitude of the two gaps. The qualitative features are the same in Fig. 5 a) and b), but they are quantitatively more pronounced in the chiral p -wave symmetry case. This may be due to the fact that the chiral p -wave gap has a constant magnitude ($|\chi(\theta)| = 1$), while the p_x -wave gap varies in magnitude upon traversing around the Fermi surface. Therefore, the LDOS is more strongly affected in the chiral p -wave case.

We now study the resolution of the LDOS in real space for a fixed energy in Fig. 6. We have chosen $R = 2$, corresponding to $h/\mu \simeq 0.14$ and also chosen the line node symmetry $\chi(\theta) = \cos \theta$. In all cases, the plots in Fig. 6 display a two-fold spatial symmetry, in accordance with the superconducting order parameter.^{23,29,30} The zero-energy peak present for $\varepsilon = 0$ evolves into a dip-structure at the vortex core upon increasing the quasiparticle energy. The deviation from the normal-state LDOS is still significant even at distances $\sim 2\xi$ away from the vortex core around $\varepsilon/\Delta_{\uparrow,0} = 0.5$. The qualitative features are the same for the chiral p -wave symmetry in Fig. 7, although the symmetry is now circular due to the isotropy of the magnitude of the gap ($|\chi(\theta)| = 1$)

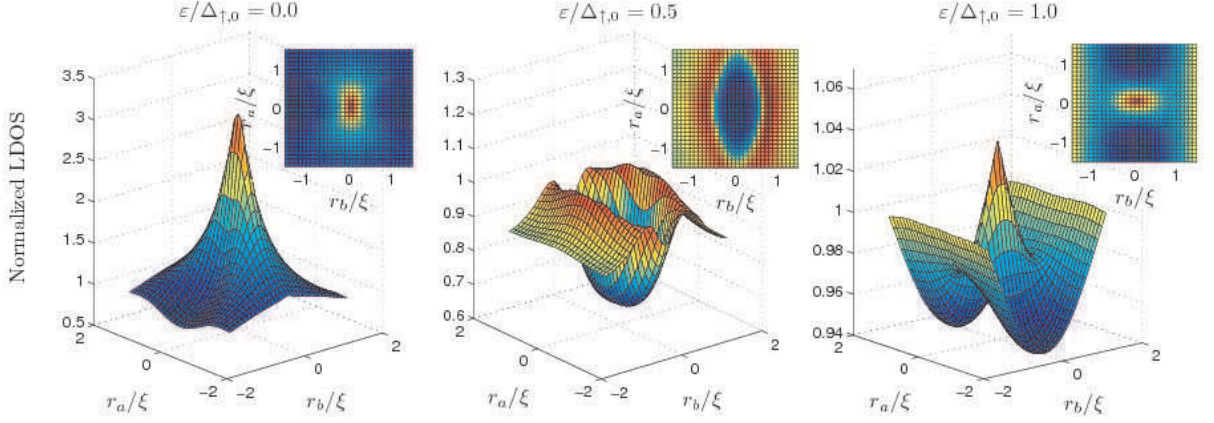


FIG. 6: (Color online) Normalized LDOS in the vicinity of the vortex core at three different quasiparticle energies, using $R = 2$ with a p_x -wave symmetry [$\chi(\theta) = \cos \theta$]. A two-fold symmetry is observed in agreement with the symmetry of the order parameter.

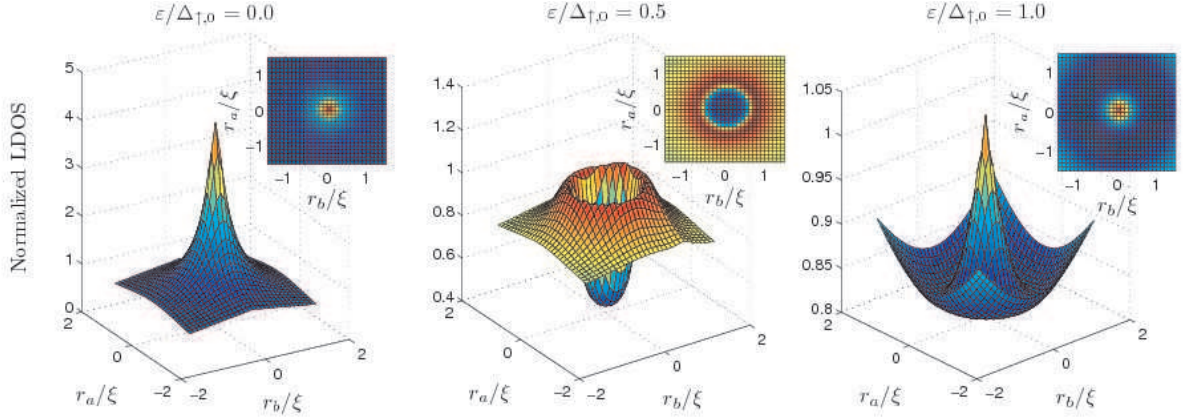


FIG. 7: (Color online) Normalized LDOS in the vicinity of the vortex core at three different quasiparticle energies, using $R = 2$ with a chiral p -wave symmetry [$\chi(\theta) = e^{i\theta}$]. A circular symmetry is observed in agreement with the symmetry of the order parameter.

IV. DISCUSSION

In our calculations, we have chosen a real gauge for both superconducting order parameters Δ_σ , $\sigma = \uparrow, \downarrow$. If the two spin-bands are completely independent, there is no phase-locking between the order parameters which fixes the relative phase $\Delta\nu = \nu_\uparrow - \nu_\downarrow$, where ν_σ is phase associated with the broken U(1) symmetry. The existence of two such phases would imply that a $U(1) \times U(1)$ symmetry is broken in a ferromagnetic superconductor, and would in principle allow for two critical temperatures which may differ in magnitude. However, if the two spin-bands do communicate by means of *e.g.* spin-orbit coupling or impurity scattering, a term of the form $-\lambda \cos(\Delta\nu)$ will appear in the free energy describing the sys-

tem. This corresponds to a phase-locking scenario where the sign of λ determines whether $\Delta\nu = 0$ or $\Delta\nu = \pi$ is the energetically preferred relative phase. Above, we have decoupled the two spin-bands such that the relative phase of Δ_\uparrow and Δ_\downarrow is of no consequence. Taking into account scattering between the spin-bands would require solving coupled Riccati-equations and investigating the effect of phase-locking explicitly, which is beyond the scope of this paper.

In Fig. 5, we plotted the relative contribution from the two spin-bands to the LDOS near the vortex core to clarify how the LDOS may give decisive clues about whether both spin bands partake in the superconducting pairing or not. In principle, it might be possible to probe explicitly the spin-resolved LDOS by using a strong ferromagnetic STM and contrasting parallel

and antiparallel relative configuration of the exchange fields in the FMSC and the ferromagnetic STM tip. The experimental realization of this particular proposal is nevertheless probably challenging.

V. SUMMARY

In summary, we have numerically studied the local density of states (LDOS) in the vicinity of a vortex core in a ferromagnetic superconductor. Specifically, we have investigated what influence the exchange field and the symmetry of the superconducting order parameter exhibit on both the spatially resolved and energy-resolved LDOS. The symmetry of the spatially resolved LDOS near the vortex core as revealed by STM-measurements should give decisive clues about the orbital symmetry of the superconducting order parameter,^{23,29,30} while the energy-resolved LDOS could provide important information about the presence of multiple gaps in the system. Our results should be comparable to experimentally obtained data, both qualitatively and quantitatively, and may thus be helpful in clarifying the nature of the superconducting pairing in ferromagnetic superconductors.

Acknowledgments

J.L. acknowledges A. Nevidomskyy for useful discussions. J.L. and A.S. were supported by the Norwegian Research Council Grant Nos. 158518/431, 158547/431, (NANOMAT), and 167498/V30 (STORFORSK). T.Y. acknowledges support by the JSPS.

APPENDIX A: MATRICES AND QUASICLASSICAL THEORY

The matrices used in this paper are defined as³¹

$$\begin{aligned} \underline{\tau}_1 &= \begin{pmatrix} 0 & 1 \\ 1 & 0 \end{pmatrix}, \quad \underline{\tau}_2 = \begin{pmatrix} 0 & -1 \\ 1 & 0 \end{pmatrix}, \quad \underline{\tau}_3 = \begin{pmatrix} 1 & 0 \\ 0 & -1 \end{pmatrix}, \\ \underline{1} &= \begin{pmatrix} 1 & 0 \\ 0 & 1 \end{pmatrix}, \quad \hat{1} = \begin{pmatrix} \underline{1} & \underline{0} \\ \underline{0} & \underline{1} \end{pmatrix}, \quad \hat{\tau}_i = \begin{pmatrix} \underline{\tau}_i & \underline{0} \\ \underline{0} & \underline{\tau}_i \end{pmatrix}, \\ \hat{\rho}_1 &= \begin{pmatrix} \underline{0} & \underline{\tau}_1 \\ \underline{\tau}_1 & \underline{0} \end{pmatrix}, \quad \hat{\rho}_2 = \begin{pmatrix} \underline{0} & -i\underline{\tau}_1 \\ i\underline{\tau}_1 & \underline{0} \end{pmatrix}, \quad \hat{\rho}_3 = \begin{pmatrix} \underline{1} & \underline{0} \\ \underline{0} & -\underline{1} \end{pmatrix}. \end{aligned} \quad (\text{A1})$$

Let us briefly sketch the way to obtain the quasiclassical Eilenberger equations for a non-unitary, spin-triplet superconducting state coexisting with ferromagnetism. For further background information on the quasiclassical theory of superconductivity, the reader may consult *e.g.* Refs. 32,33,34,35,36

for nice reviews. We follow here closely the notation of Ref.³¹. Our starting point is the following Hamiltonian:

$$\begin{aligned} H &= \sum_{\alpha\beta} \int d\mathbf{r} \psi_{\alpha}^{\dagger}(\mathbf{r}, t) \left(-\frac{\nabla^2}{2m} \underline{1} - h\underline{\tau}_3 \right)_{\alpha\beta} \psi_{\beta}(\mathbf{r}, t) \\ &\quad - \sum_{\sigma} \int d\mathbf{r} d\mathbf{r}' [\Delta_{\sigma}(\mathbf{r}, \mathbf{r}') \psi_{\sigma}^{\dagger}(\mathbf{r}) \psi_{\sigma}^{\dagger}(\mathbf{r}') \\ &\quad + \Delta_{\sigma}^{*}(\mathbf{r}, \mathbf{r}') \psi_{\sigma}(\mathbf{r}') \psi_{\sigma}(\mathbf{r})]. \end{aligned} \quad (\text{A2})$$

The Heisenberg equation of motion for the above Hamiltonian is obtained in the standard way:

$$\begin{aligned} i\partial_t \hat{\rho}_3 \Psi(\mathbf{r}, t) &= \int d\mathbf{r}' \hat{H}(\mathbf{r}, \mathbf{r}', t) \Psi(\mathbf{r}, t), \\ \hat{H}(\mathbf{r}, \mathbf{r}', t) &= \hat{\xi}(\mathbf{r}) \delta(\mathbf{r} - \mathbf{r}') - \hat{\Delta}(\mathbf{r}, \mathbf{r}'), \quad \hat{\xi}(\mathbf{r}) = -\frac{\nabla_{\mathbf{r}}^2}{2m} \hat{1}, \\ \hat{\Delta}(\mathbf{r}, \mathbf{r}') &= \begin{pmatrix} \underline{0} & \underline{\Delta}(\mathbf{r}, \mathbf{r}') \\ \underline{\Delta}^{*}(\mathbf{r}, \mathbf{r}') & \underline{0} \end{pmatrix}, \\ \underline{\Delta}(\mathbf{r}, \mathbf{r}') &= \text{diag}[\Delta_{\uparrow}(\mathbf{r}, \mathbf{r}'), \Delta_{\downarrow}(\mathbf{r}, \mathbf{r}')]. \end{aligned} \quad (\text{A3})$$

For simplicity, we consider only the retarded component of the Green's function G^{R} in what follows, since the system is specified exclusively by G^{R} in an equilibrium situation. It is defined as

$$\underline{G}_{\alpha\beta}^{\text{R}}(1, 2) = -i\Theta(t_1 - t_2) \langle [\psi_{\alpha}(1), \psi_{\beta}^{\dagger}(2)]_{+} \rangle, \quad (\text{A4})$$

where the notation $(1, 2)$ refers to the spatial and time coordinates: $(1) \equiv (\mathbf{r}_1; t_1)$. We explicitly write the '+' sign as a subscript to denote an anticommutator; it is else implicitly understood that the notation [...] denotes a usual commutator. Similarly, the anomalous Green's function is given by

$$\underline{F}_{\alpha\beta}^{\text{R}}(1, 2) = -i\Theta(t_1 - t_2) \langle [\psi_{\alpha}(1), \psi_{\beta}(2)]_{+} \rangle. \quad (\text{A5})$$

One may construct 4×4 matrices in combined particle-hole and spin space, known as Nambu space, in the following manner:

$$\hat{G}^{\text{R}}(1, 2) = \begin{pmatrix} \underline{G}^{\text{R}}(1, 2) & \underline{F}^{\text{R}}(1, 2) \\ [\underline{F}^{\text{R}}(1, 2)]^{*} & [\underline{G}^{\text{R}}(1, 2)]^{*} \end{pmatrix}. \quad (\text{A6})$$

Note that $G(1, 2)$ is a generalized Gor'kov Green's function, which contains information about processes occurring at length scales comparable to the Fermi wavelength. Such information is lost upon applying the quasiclassical approximation. Using the Heisenberg equation of motion Eq. (A3), we obtain

$$\left[{}_1\partial_{t_1} \left(\hat{\rho}_3 \hat{G}^R(1, 2) \right)_{ij} - \int d\mathbf{r}' \sum_l [-1\Theta(t_1 - t_2)] \hat{H}_{il}(\mathbf{r}_1, \mathbf{r}', t_1) (\hat{\rho}_3)_{ll} \langle [\Psi_l(\mathbf{r}', t_1), \Psi_j^\dagger(\mathbf{r}_2, t_2)]_+ \rangle \right] = \delta_{ij} \delta(1 - 2). \quad (\text{A7})$$

To arrive at Eq. (1), it is convenient to introduce the mixed representation which shifts the frame of reference to a center-of-mass system. We define

$$\begin{aligned} \mathbf{R} &= (\mathbf{r}_1 + \mathbf{r}_2)/2, \quad \mathbf{r} = \mathbf{r}_1 - \mathbf{r}_2, \\ T &= (t_1 + t_2)/2, \quad t = t_1 - t_2, \end{aligned} \quad (\text{A8})$$

such that

$$\hat{G}^R(1, 2) = \hat{G}^R(\mathbf{R} + \frac{\mathbf{r}}{2}, T + \frac{t}{2}, \mathbf{R} - \frac{\mathbf{r}}{2}, T - \frac{t}{2}). \quad (\text{A9})$$

The Fourier-transformation of Eq. (A9) yields

$$\hat{G}^R(\mathbf{p}, \mathbf{R}; T, \varepsilon) = \int d\mathbf{r} e^{-i\mathbf{p}\mathbf{r}} \int dt e^{it\varepsilon} \hat{G}^R(1, 2). \quad (\text{A10})$$

An exact solution for $\hat{G}^R(\mathbf{p}, \mathbf{R}; T, \varepsilon)$ is very hard to achieve, but the situation is considerably simplified if one is willing to neglect all atomic-scale fine structure effects that are included in \hat{G}^R . These give rise to a rapidly oscillating part in the solution for \hat{G}^R , and rewriting the Green's function through Eq. (A10) allows us to integrate out this unnecessary information (at least for our purposes). This approximation may be expected to yield satisfactory results if the energy of the physical quantities involved in the problem, *e.g.* exchange field and superconducting order parameter, are much smaller than the Fermi energy. Assuming that only particles in the vicinity of Fermi level will take part in physical processes, one only needs to retain the direction of the momentum at Fermi level in the \mathbf{p} coordinate.

As this Appendix is only meant as background information for the Eilenberger equation, we do not show all the details leading from Eq. (A7) to Eq. (1) here. The calculations are nevertheless fairly straight-forward, and consist of first switching to a mixed representation, then Fourier-transforming the variables, and finally performing the quasi-classical approximation

$$\hat{g}^R = \frac{1}{\pi} \int d\xi_{\mathbf{p}} \hat{G}^R, \quad \xi_{\mathbf{p}} = \frac{\mathbf{p}^2}{2m}. \quad (\text{A11})$$

APPENDIX B: INELASTIC SCATTERING

The choice of $\delta = 0.1\Delta_{\uparrow,0}$ is motivated by the fact that the zero-energy peaks observed in experiments are usually limited from above to roughly a factor of five times the normal-state value of the LDOS, which we reproduce with this particular choice of δ . Choosing δ smaller (corresponding to a longer quasiparticle lifetime since $\delta = \tau^{-1}$) causes the zero-energy peak to grow substantially, as shown in Fig. 8. In general, the inelastic scattering rate does not have to be proportional to the gap at all and our choice of $\delta = 0.1\Delta_{\uparrow,0}$ is simply chosen to compare the scattering rate against a familiar quantity.

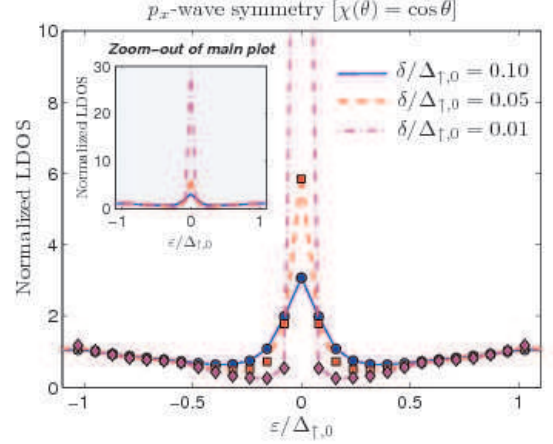


FIG. 8: (Color online) Normalized LDOS in the vicinity of the vortex core at three different values of the inelastic scattering rate $\delta = \tau^{-1}$, using a p_x -wave symmetry with $h/\mu = 0.15$.

APPENDIX C: DERIVATION OF EQ. (14)

The gap equation may be obtained by starting out with a Hamiltonian assuming a non-unitary triplet pairing state co-existing with itinerant ferromagnetism^{7,18}, namely

$$\begin{aligned} \hat{H} &= \sum_{\mathbf{k}} \xi_{\mathbf{k}} + \frac{INM^2}{2} - \frac{1}{2} \sum_{\mathbf{k}\sigma} \Delta_{\mathbf{k}\sigma}^\dagger b_{\mathbf{k}\sigma\sigma} \\ &+ \frac{1}{2} \sum_{\mathbf{k}\sigma} \left(\hat{c}_{\mathbf{k}\sigma}^\dagger \hat{c}_{-\mathbf{k}\sigma} \right) \begin{pmatrix} \xi_{\mathbf{k}\sigma} & \Delta_{\mathbf{k}\sigma\sigma} \\ \Delta_{\mathbf{k}\sigma\sigma}^\dagger & -\xi_{\mathbf{k}\sigma} \end{pmatrix} \begin{pmatrix} \hat{c}_{\mathbf{k}\sigma} \\ \hat{c}_{-\mathbf{k}\sigma}^\dagger \end{pmatrix}, \end{aligned} \quad (\text{C1})$$

Here, I is the ferromagnetic exchange coupling constant, N is the number of lattice sites, M denotes the magnetic order parameter (dimensionless), while $b_{\mathbf{k}\sigma\sigma}$ is the Cooper pair expectation value. Diagonalization of this Hamiltonian produces:

$$\begin{aligned} \hat{H} &= H_0 + \sum_{\mathbf{k}\sigma} E_{\mathbf{k}\sigma} \hat{\gamma}_{\mathbf{k}\sigma}^\dagger \hat{\gamma}_{\mathbf{k}\sigma}, \\ H_0 &= \frac{1}{2} \sum_{\mathbf{k}\sigma} (\xi_{\mathbf{k}\sigma} - E_{\mathbf{k}\sigma} - \Delta_{\mathbf{k}\sigma\sigma}^\dagger b_{\mathbf{k}\sigma\sigma}) + \frac{INM^2}{2}, \end{aligned} \quad (\text{C2})$$

where $\{\hat{\gamma}_{\mathbf{k}\sigma}, \hat{\gamma}_{\mathbf{k}\sigma}^\dagger\}$ are new fermion operators and the eigenvalues read

$$E_{\mathbf{k}\sigma} = \sqrt{\xi_{\mathbf{k}\sigma}^2 + |\Delta_{\mathbf{k}\sigma\sigma}|^2}. \quad (\text{C3})$$

Above, $\xi_{\mathbf{k}}$ is the kinetic energy measured from Fermi level. By minimizing the free energy, one obtains the gap equation

for the superconducting order parameter:⁷

$$\Delta_{\mathbf{k}\sigma\sigma} = -\frac{1}{N} \sum_{\mathbf{k}'} V_{\mathbf{k}\mathbf{k}'\sigma\sigma} \frac{\Delta_{\mathbf{k}'\sigma\sigma}}{2E_{\mathbf{k}'\sigma}} \tanh(\beta E_{\mathbf{k}'\sigma}/2). \quad (\text{C4})$$

Assuming that the gap is fixed on the Fermi surface in the weak-coupling limit, one may write in general

$$V_{\sigma\sigma}(\theta, \theta') = -V_0 Y^\sigma(\theta) [Y^\sigma(\theta')]^*. \quad (\text{C5})$$

where $Y^\sigma(\theta)$ are basis functions for the angular dependence of the interaction. To model p_x -wave and chiral p -wave pairing, respectively, we use $Y^\sigma(\theta) = -\sigma e^{i\sigma\theta}$ and $Y^\sigma(\theta) = \cos\theta$. Conversion to integral gap equations is accomplished by means of the identity

$$\frac{1}{N} \sum_{\mathbf{k}} f(\xi_{\mathbf{k}\sigma}) = \int d\varepsilon N^\sigma(\varepsilon), \quad (\text{C6})$$

where $N^\sigma(\varepsilon)$ is the spin-resolved density of states. In three spatial dimensions, this may be calculated from the dispersion relation by using the formula

$$N^\sigma(\varepsilon) = \frac{V}{(2\pi)^3} \int_{\varepsilon_{\mathbf{k}\sigma} = \text{const}} \frac{dS_{\varepsilon_{\mathbf{k}\sigma}}}{|\hat{\nabla}_{\mathbf{k}} \varepsilon_{\mathbf{k}\sigma}|}. \quad (\text{C7})$$

With the dispersion relation $\xi_{\mathbf{k}\sigma} = \varepsilon_{\mathbf{k}} - \sigma IM - \mu$, one obtains

$$N^\sigma(\varepsilon) = \frac{mV \sqrt{2m(\varepsilon + \sigma IM + \mu)}}{2\pi^2}. \quad (\text{C8})$$

In their integral form, the gap equation reads

$$1 = \frac{V_0}{4\pi} \sum_{\sigma} \int_{-\omega_0}^{\omega_0} d\varepsilon \frac{N^\sigma(\varepsilon) Y^\sigma(\theta) [Y^\sigma(\theta')]^*}{E_\sigma(\varepsilon)} \tanh[\beta E_\sigma(\varepsilon)/2]. \quad (\text{C9})$$

Consider now $T = 0$, where the integral may be done analytically to yield:

$$\Delta_{\sigma,0} = c\omega_0 e^{-1/g\sqrt{1+\sigma\tilde{M}}}, \quad \sigma = \uparrow, \downarrow \quad (\text{C10})$$

where we have defined $\tilde{M} = IM/\mu = \hbar/\mu$, i.e. the exchange energy scaled on the Fermi energy. Moreover, c is a numerical prefactor which depends on which symmetry one considers (p_x -wave or chiral p -wave) while g is the weak-coupling constant. The important influence of the magnetization is that it modifies the density of states, which affects the superconductivity gaps. For $\tilde{M} = 1$, i.e. an exchange splitting equal to the Fermi energy, the minority spin gap is completely suppressed. Thus, the presence of magnetization reduces the available phase space for the minority spin Cooper pairs, suppressing the gap and the critical temperature compared to the pure Bardeen-Cooper-Schrieffer case.

-
- ¹ N.T. Huy, A. Gasparini, D.E. de Nijs, Y. Huang, J.C.P. Klaasse, T. Gortenmulder, A. de Visser, A. Hamann, T. Gorlach, H. v. Lohneysen, Phys. Rev. Lett. **99**, 067006 (2007).
 - ² S. S. Saxena, P. Agarwal, K. Ahilan, F. M. Grosche, R. K. W. Haselwimmer, M. J. Steiner, E. Pugh, I. R. Walker, S. R. Julian, P. Monthoux, G. G. Lonzarich, A. Huxley, I. Sheikin, D. Braithwaite, and J. Flouquet, Nature **406**, 587 (2000).
 - ³ D. Aoki, A. Huxley, E. Ressouche, D. Braithwaite, J. Flouquet, J.-P. Brison, E. Lhotel, and C. Paulsen, Nature **413**, 613 (2001).
 - ⁴ R. Shen, Z. M. Zheng, S. Liu, and D. Y. Xing, Phys. Rev. B **67**, 024514 (2003).
 - ⁵ K. V. Samokhin and M. B. Walker, Phys. Rev. B **66**, 174501 (2002); K. V. Samokhin and M. B. Walker, Phys. Rev. B **66**, 024512 (2002); M. B. Walker and K. V. Samokhin, Phys. Rev. Lett. **88**, 207001 (2002).
 - ⁶ A. Harada, S. Kawasaki, H. Mukuda, Y. Kitaoka, Y. Haga, E. Yamamoto, Y. Onuki, K. M. Itoh, E. E. Haller, H. Harima, Phys. Rev. B **75**, 140502 (2007).
 - ⁷ A. H. Nevidomskyy, Phys. Rev. Lett. **94**, 097003 (2005).
 - ⁸ J. Linder and A. Sudbø, Phys. Rev. B **76**, 054511 (2007).
 - ⁹ J. Linder, I. B. Sperstad, A. Nevidomskyy, M. Cuoco, and A. Sudbø, Phys. Rev. B **77**, 184511 (2008).
 - ¹⁰ D. V. Shopova and D. I. Uzunov, Phys. Rev. B **72**, 024531 (2005).
 - ¹¹ D. I. Uzunov, Europhys. Lett. **77**, 20008 (2007); D. I. Uzunov, Phys. Rev. B **74**, 134514 (2006).
 - ¹² S. Tewari, D. Belitz, T. R. Kirkpatrick, and J. Toner, Phys. Rev. Lett. **93**, 177002 (2004).
 - ¹³ L. Radzihovsky, A. M. Ettouhami, K. Saunders, and J. Toner, Phys. Rev. Lett. **87**, 027001 (2001).
 - ¹⁴ A. Knigavko and B. Rosenstein, Phys. Rev. B **58**, 9354 (1998).
 - ¹⁵ V. P. Mineev, cond-mat/0507572.
 - ¹⁶ A. Brataas and Y. Tserkovnyak, Phys. Rev. Lett. **93**, 087201 (2004).
 - ¹⁷ Y. Zhao and R. Shen, Phys. Rev. B **73**, 214511 (2006).
 - ¹⁸ M. S. Grønsløth, J. Linder, J.-M. Børven, and A. Sudbø, Phys. Rev. Lett. **97**, 147002 (2006); J. Linder, M. S. Grønsløth, and A. Sudbø, Phys. Rev. B **75**, 024508 (2007).
 - ¹⁹ J. Linder, M. S. Grønsløth, and A. Sudbø, Phys. Rev. B **75**, 054518 (2007).
 - ²⁰ T. Yokoyama and Y. Tanaka, Phys. Rev. B **75**, 132503 (2007).
 - ²¹ H. F. Hess, R. B. Robinson, R. C. Dynes, J. M. Valles, Jr., and J. V. Waszczak, Phys. Rev. Lett. **62**, 214 (1989).
 - ²² G. Eilenberger, Z. Phys. **214**, 195 (1968).
 - ²³ N. Schopohl and K. Maki, Phys. Rev. B **52**, 490 (1995); N. Schopohl, cond-mat/9804064.
 - ²⁴ M. Eschrig, Phys. Rev. B **61**, 9061 (2000).
 - ²⁵ Z. Tesanovic, Phys. Rev. B **59**, 6449 (1999).
 - ²⁶ A. K. Nguyen and A. Sudbø, Phys. Rev. B **60**, 15307 (1999); Europhys. Lett., **46**, 780 (1999).
 - ²⁷ T. Yokoyama, Y. Tanaka, A. A. Golubov, Phys. Rev. B **78**, 012508 (2008).
 - ²⁸ C. Caroli, P. G. de Gennes, and J. Matricon, Phys. Lett. **9**, 307 (1964).
 - ²⁹ H. F. Hess, R. B. Robinson, and J. V. Waszczak, Phys. Rev. Lett. **64** 2711 (1990).
 - ³⁰ M. Ichioka, N. Hayashi, N. Enomoto, and K. Machida Phys. Rev.

- B **53**, 15316 (1996).
- ³¹ We will use the notations and conventions of J. P. Morten, Master Thesis, Norwegian University of Science and Technology, (2003) (unpublished), which in turn is close the notations used in Ref. 32.
- ³² J. W. Serene and D. Rainer, Phys. Rep. **101**, 221 (1983).
- ³³ N. Kopnin, *Theory of Nonequilibrium Superconductivity*, (Oxford University Press, New York, 2001).
- ³⁴ J. Rammer and H. Smith, Rev. Mod. Phys. **58**, 323 (1986).
- ³⁵ A. M. Zagorin, *Quantum Theory of Many-Body Systems*, Springer, 1998.
- ³⁶ V. Chandrasekhar, in *The Physics of Superconductors*, Vol II, edited by K.-H. Bennemann and J. B. Ketterson, Springer-Verlag, Berlin (2004); arXiv:cond-mat/0312507.